



Mechanism of fluorophore quenching in a pre-fluorescent nitroxide probe: A theoretical illustration



Carolina Aliaga^{a,b,*}, Patricio Fuentealba^{b,c}, Marcos Caroli Rezende^a, Carlos Cárdenas^{b,c}

^a Facultad de Química y Biología, Universidad de Santiago de Chile, Casilla 40, Correo 33, Santiago, Chile

^b Center for the Development of Nanoscience and Nanotechnology CEDENNA, Av. Ecuador 3493, 917-0124 Santiago, Chile

^c Facultad de Ciencias, Universidad de Chile, Las Palmeras 3425, Ñuñoa, Santiago, Chile

ARTICLE INFO

Article history:

Received 4 October 2013

In final form 20 December 2013

Available online 7 January 2014

ABSTRACT

The mechanism of fluorophore quenching in QT, a pre-fluorescent quinoline-TEMPO probe, is illustrated with the aid of a molecular-orbital analysis, offering a pictorial view of the process that takes place in the excited molecule, and which is responsible for the observed fluorescence quenching.

© 2014 Elsevier B.V. All rights reserved.

1. Introduction

Paramagnetic nitroxides are well known as efficient quenchers of singlet-excited states of fluorophores [1–3]. The quenching is even more efficient if the fluorophore is covalently linked to the nitroxide, converting this interaction to an intramolecular process [2,4–6].

In 1988 Blough and Simpson took advantage of this effect to design for the first time a sensitive probe for monitoring hydrogen-transfer reactions [7]. By linking covalently a fluorophore to a nitroxide moiety, a hybrid molecule was built that acted as a paramagnetic ‘pre-fluorescent’ probe, where fluorescence is quenched by the radical fragment and restored by the annihilation of the paramagnetic moiety when a hydrogen atom is transferred. Since the disappearance of the radical nitroxide is concomitant with the restoration of the probe fluorescence, the process can be monitored by both fluorescence and/or electron paramagnetic resonance spectroscopy. Thus, the use of pre-fluorescent probes has become a powerful and versatile tool to monitor *in situ* biological processes mediated by free-radical species [8–12].

The fluorophore quenching by the nitroxide radical is commonly interpreted as arising from an intramolecular electron-exchange interaction between the fluorophore and the radical fragment. Photophysical measurements support this view [10], which has been theoretically rationalized with the aid of qualitative diagrams [4]. However, to the best of our knowledge, a detailed theoretical description of the orbitals involved in the quenching process is not available in the literature.

In the present Letter we carried out calculations on the pre-fluorescent probe 4-(3-hydroxy-2-methyl-4-quinolinoyloxy)-2,2,6,6-tetramethylpiperidine-1-oxyl free radical (QT) derived from a

quinoline fluorophore covalently linked to a nitroxide (TEMPO) moiety, which has been used as a radical scavenger and a hydrogen-abstractor in a variety of applications [10,11]. To explain the fact that the added hydrogen atom to the QT species restores the fluorescence we have done theoretical calculations of the spectra and an analysis of the molecular orbitals involved in the process (Scheme 1).

2. Materials and methods

2.1. Experimental

The UV–Vis spectrum was recorded with a Perkin Elmer Lambda 40 spectrophotometer; the fluorescence spectrum of the QT probe was measured at room temperature with a Perkin Elmer LS 55 spectrophotometer.

The 4-(3-hydroxy-2-methyl-4-quinolinoyloxy)-2,2,6,6-tetramethylpiperidine-1-oxyl free radical (QT) was prepared as reported previously [13].

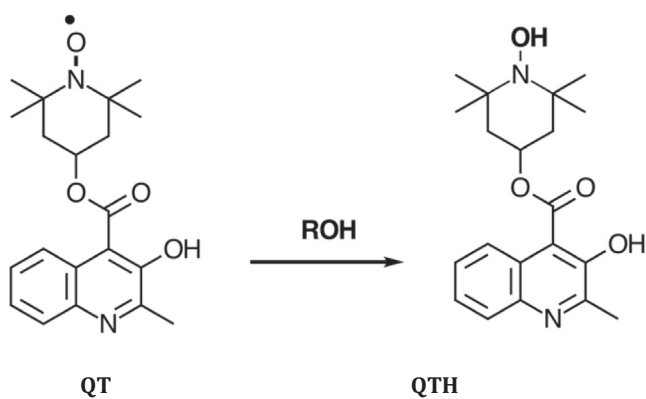
2.2. Theoretical calculations

All calculations were performed with the GAUSSIAN 09 package [14]. Given the size of the molecules studied here, reliable but expensive computational wave-function-based *ab initio* methods, such as coupled clusters or configuration interaction, were ruled out to compute excited states. However, for the calculation of the electronic spectra TD-DFT methods have shown to be accurate enough and computationally accessible for medium and big molecules.

In this Letter, the geometry of all molecules was first optimized using the functional B3LYP along with the 6-311++G(d,p) basis set. Then, all harmonic vibrational frequencies were computed to be sure that the optimized structures were actual stable minima. In no case an imaginary frequency was found. In order to include

* Corresponding author at: Facultad de Química y Biología, Universidad de Santiago de Chile, Casilla 40, Correo 33, Santiago, Chile.

E-mail address: carolina.aliaga@usach.cl (C. Aliaga).



possible long-range interactions in the ground or in the excited states, all the structures were re-optimized, starting from the B3LYP calculation, with the long-range corrected CAM-B3LYP functional and the same basis set. In all cases, the first three vertical excited states of singlet and triplet spin symmetries were computed using the GAUSSIAN 09 code [14]. The most important Kohn–Sham molecular orbitals obtained from the last calculations were then analyzed.

Solvent effects on the absorption spectra of all molecules were simulated with the aid of the polarized-continuum-model (PCM) option.

3. Results and discussion

QT is a pre-fluorescent probe that absorbs at 330 nm in acetonitrile. The λ_{max} value of this absorption band changes slightly with the solvent, with a small bathochromic shift (<10 nm) in more polar solvents. Its emission band is quenched by the paramagnetic nitroxide radical, but reappears when this fragment abstracts a hydrogen atom to form QTH, a diamagnetic hydroxylamine [10]. Both QT and QTH exhibit practically the same absorption spectrum in acetonitrile (Figure 1). This observation reflects the fact that, as occurs for a variety of probes with a nitroxide radical, the probe absorption is essentially due to the fluorophore and is not affected by the radical fragment [12].

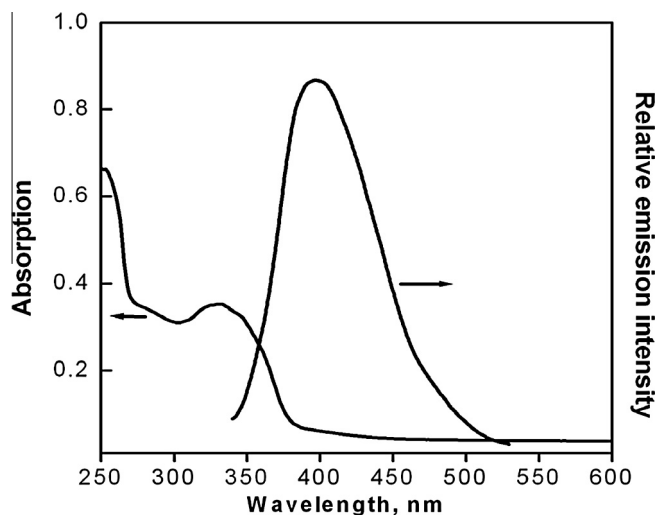


Figure 1. QT absorption and QTH emission band in acetonitrile (ca 20 mM). The sample was excited at 330 nm for the fluorescence spectrum.

TD-DFT calculations for QT and QTH yielded similar transitions. QT showed an $S_0 \rightarrow S_1$ absorption at 304 nm ($f = 0.16$), corresponding to a HOMO–1 \rightarrow LUMO transition. QTH showed an $S_0 \rightarrow S_1$ absorption at 304 nm ($f = 0.16$) in the gas phase, corresponding to a HOMO \rightarrow LUMO transition. In addition, it exhibited a second transition at 287 nm corresponding to a singlet excitation from HOMO–1 \rightarrow LUMO ($f = 0.12$).

These values did not change appreciably when the effect of the solvent was taken into account. By carrying out calculations with the polarizable continuum model an estimated λ_{max} value of 307 nm ($f = 0.20$) was obtained for QT and a value of 306 nm ($f = 0.20$) was estimated for QTH in methanol.

3.1. Frontier molecular orbitals of QT

The HOMO–1 (–0.28819 a.u.) and the SOMO (–0.27136 a.u.) are rather close in energy, with an energy difference of 0.46 eV, much smaller than the difference between the LUMO and the HOMO–1 (6.7 eV) of QT. Figure 2 depicts isosurfaces for the frontier molecular orbitals of QT. The HOMO–1 and the LUMO are both centered on the quinoline moiety, unlike the SOMO, which is entirely concentrated on the nitroxide radical fragment. Thus, the overlap between the HOMO–1 and the LUMO is favorable and the corresponding electric-dipole-transition matrix should be different from zero, giving rise to the allowed HOMO–1 \rightarrow LUMO transition. By contrast, overlap between the SOMO and the LUMO is negligible and a SOMO \rightarrow LUMO transition is not allowed.

3.2. Frontier molecular orbitals of QTH

Figure 2 shows the isosurfaces for the frontier molecular orbitals (HOMO–1, HOMO and LUMO) of QTH. All of these orbitals are centered on the quinoline moiety. The good overlap between them leads to allowed transitions from the HOMO–1 and the HOMO to the LUMO. In addition, visual inspection of these orbitals readily correlates the LUMO of QTH with the LUMO of QT, and the HOMO of QTH with the HOMO–1 of QT.

The energy levels of the frontier orbitals of QTH and QT are compared in Figure 3. Their relative values again establish a correlation between the LUMO's of both species, and between the HOMO of QTH and the HOMO–1 of QT. Thus, the main difference between the frontier orbitals of QTH and QT is the intercalation, in the latter, of a SOMO orbital (centered on the nitroxide moiety, see Figure 2) between what were originally the energy levels of the HOMO and the LUMO of QTH.

The HOMO \rightarrow LUMO one-electron excitation in QTH is very similar to the HOMO–1 \rightarrow LUMO excitation in QT. However, due to the intercalation of a SOMO orbital centered on the TEMPO fragment between the HOMO–1 and the LUMO of QT, the possibility now arises of an electron exchange between the LUMO and the SOMO of the excited QT (Figure 4). The energy difference between the SOMO and the LUMO is very large (0.22893 a.u., 6.23 eV), ruling out any possibility of energy-transfer between these levels. However, such large energy difference does not deter the possibility of an interaction between the unpaired spin of the SOMO and the electron of the singly-occupied LUMO of the excited QT. This interaction is responsible for the nonradiative relaxation of the excited QT, and its observed fluorescence quenching.

The isosurfaces of Figure 2 show that there is little overlap in space between the LUMO of QT and its SOMO, since these orbitals are centered on different regions of the molecule. This observation raises the question as to the effect of the distance between the quinoline chromophore and the TEMPO fragment on the quenching ability of the latter. The lack of spatial overlap between the two orbitals might suggest that the distance between the two fragments affect the spin-exchange process. To verify this, we

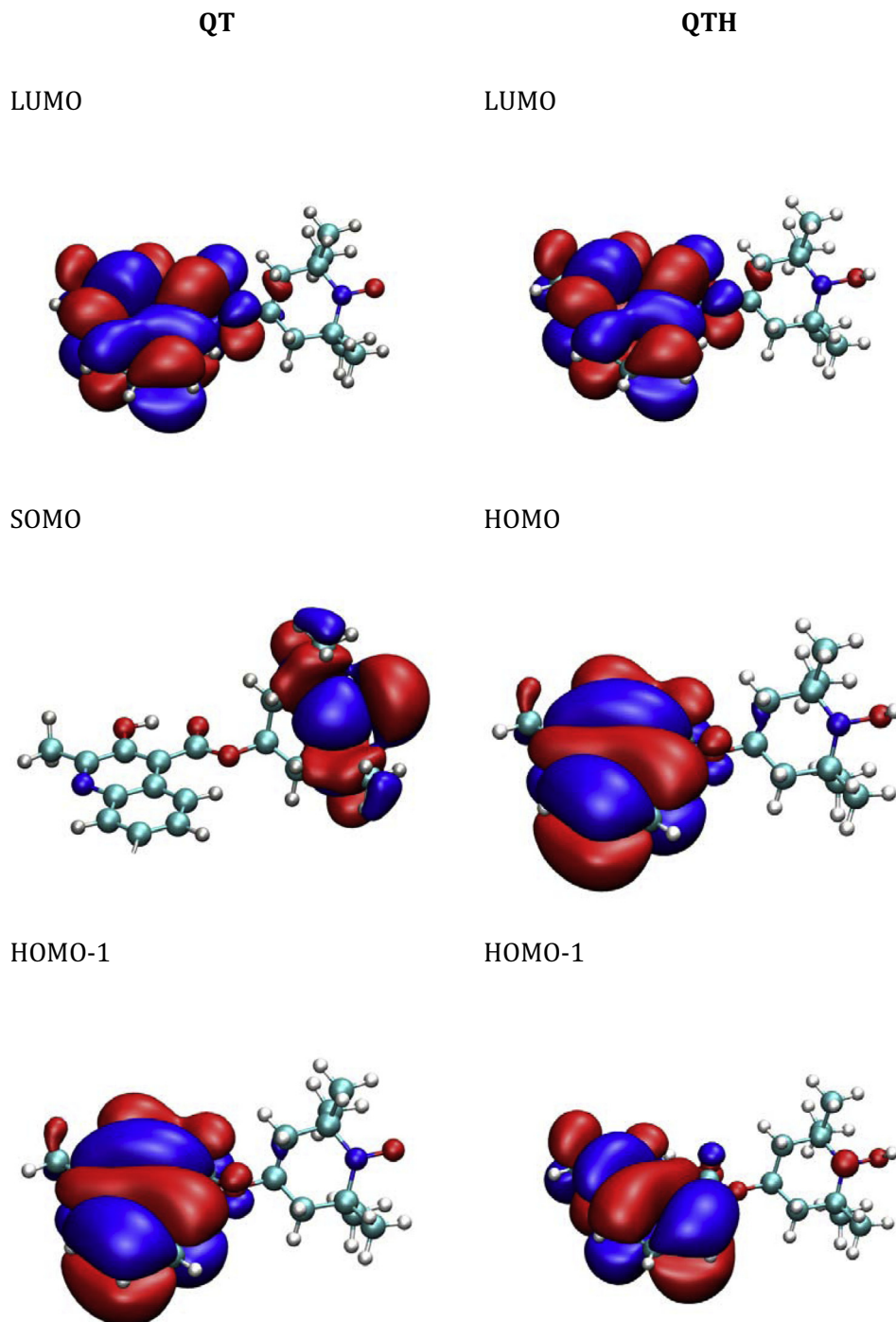


Figure 2. Frontier molecular orbitals of QT (left) and QTH (right).

performed calculations on a hypothetical molecule ($Q(\text{CH}_2)_3\text{T}$), where a saturated chain of three carbon atoms was inserted between the carboxylic group of the quinoline fluorophore (Q) and the TEMPO ring (T). Figure 5 shows the HOMO isosurface of this hypothetical molecule. It can be seen that the highest occupied molecular orbital of the system is now centered on the quinoline moiety, suggesting that the fluorescence of the chromophore could be restored when the nitroxide is further separated from it.

This observation parallels the well known fact that the quenching ability of a nitroxide radical tends to drop off when it is further removed from the fluorophore [15,16].

The above analysis follows what is commonly accepted as the mechanism of fluorescence quenching of nitroxide probes, and of fluorescence restoration when these radical probes are converted to a hydroxylamine by hydrogen abstraction [10]. The results presented here, from theoretical calculations on the particular example of the QT/QTH pair, illustrate in a more pictorial and quantitative way, a mechanism that is commonly depicted only in a qualitative way. Intercalation, between the frontier orbitals of the fluorophore, of a SOMO entirely centered on the nitroxide radical, makes possible a spin exchange between it and the LUMO of the excited fluorophore possible, leading to an efficient

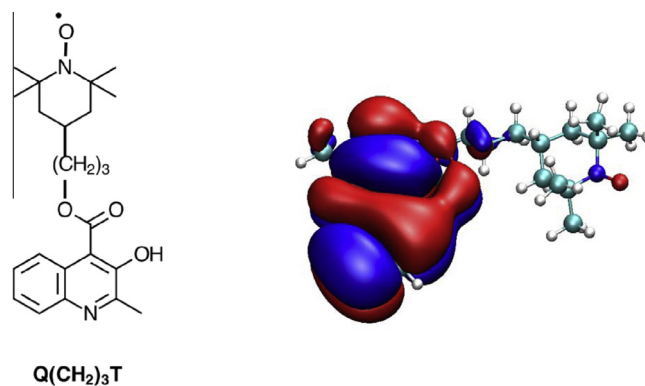
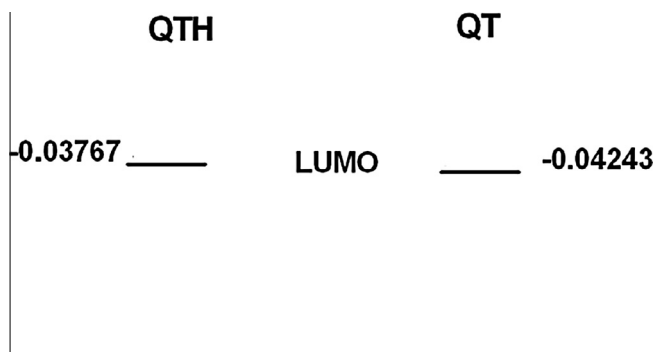


Figure 5. Structure of the hypothetical profluorescent probe $Q(CH_2)_3T$, with a propylene spacer between the quinoline fluorophore and the nitroxide (left). HOMO isosurface of $Q(CH_2)_3T$ (right).

non-radiative relaxation of the excited probe and to the observed fluorescence quenching.

Acknowledgments

This Letter has been supported by FONDECYT Projects 1110736, 1130202 and Financiamiento Basal para Centros Científicos y Tecnológicos de Excelencia FB0807.

References

- [1] J.A. Green, L.A. Singer, J.H. Parks, *J. Chem. Phys.* 58 (1973) 2690.
- [2] S.E. Herbelin, V.N. Blough, *J. Phys. Chem. B* 102 (1998) 8170.
- [3] A.R. Watkins, *Phys. Lett.* 29 (1974) 526.
- [4] J.P. Blinco, K.E. Fairfull-Smith, B.M. Morrow, S.E. Bottle, *Aust. J. Chem.* 64 (2011) 373.
- [5] S.G. Jockusch, Dedola, G. Lem, N.J. Turro, *J. Phys. Chem. B* 103 (1999) 9126.
- [6] J.A. Green, L.A. Singer, *J. Am. Chem. Soc.* 96 (1974) 2730.
- [7] V. Blough, D.J. Simpson, *J. Am. Chem. Soc.* 110 (1988) 1915.
- [8] S.S. Atik, L.A. Singer, *J. Am. Chem. Soc.* 100 (1978) 3234.
- [9] J.C. Scaiano, C.I. Paraskevopoulos, *Can. J. Chem.* 62 (1984) 2351.
- [10] C. Aliaga, A. Aspée, J.C. Scaiano, *Org. Lett.* 22 (2003) 4145.
- [11] F. Mito et al., *Free Rad. Res.* 45 (2011) 1103.
- [12] S.A. Green, D.J. Simpson, G. Zhou, P.S. Ho, N.V. Blough, *J. Am. Chem. Soc.* 112 (1990) 7337.
- [13] C. Aliaga, D.R. Stuart, A. Aspée, J.C. Scaiano, *Org. Lett.* 17 (2005) 3665.
- [14] GAUSSIAN 09, Revision A.1, M.J. Frisch, et al. Gaussian Inc, Wallingford CT, 2009.
- [15] É. Hídeg, T. Kálai, *Photochem. Photobiol.* 82 (2006) 1211.
- [16] Ch. Tansakul et al., *J. Phys. Chem. C* 114 (2010) 7793.

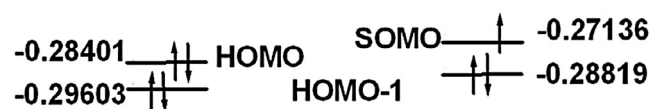


Figure 3. Comparison of the energy levels of the frontier orbitals of QT and QTH drawn in scale. Energy values are given in atomic units. The main difference between the energy levels of QTH and QT is the intercalation in the latter of a SOMO between the HOMO (HOMO-1 of QT) and the LUMO of both species.

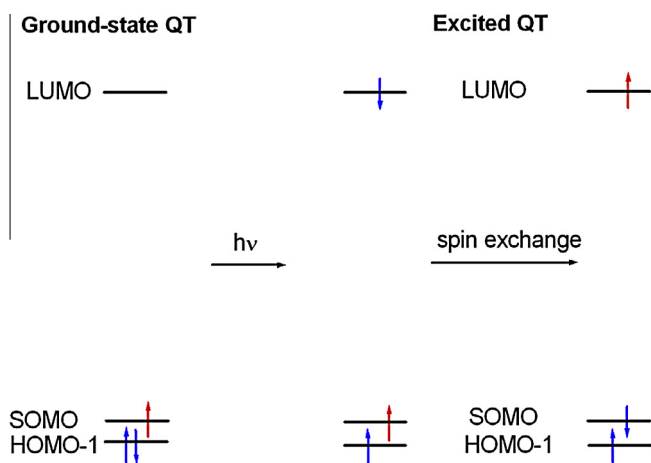


Figure 4. Energy levels for QT in the ground (left) and excited state (right), with a schematic illustration of the interaction between the unpaired spin of the nitroxide SOMO and the LUMO of the excited fluorophore.